Sanner, M., Widmer, A., Senn, H., & Braun, W. (1989) *J. Comput. Aided Mol. Des. 3*, 195-210.
Schaumann, T., Braun, W., & Wüthrich, K. (1990) *Biopolymers 29*, 679-694.
Senn, H., Werner, B., Messerle, B. A., Weber, C., Traber, R., & Wüthrich, K. (1989) *FEBS Lett. 249*, 113-118.
Senn, H., Loosli, H. R., Sanner, M., & Braun, W. (1990) *Biopolymer 29*, 1387-1400.
Takahashi, N., Hayano, T., & Suzuki, M. (1989) *Nature 337*, 437-475.
Wider, G., Weber, C., Widmer, H., Traber, H., & Wüthrich, K. (1990) *J. Am. Chem. Soc. 112*, 9015-9017.
Wider, G., Weber, C., & Wüthrich, K. (1991) *J. Am. Chem. Soc.* (in press).
Wüthrich, K. (1976) *NMR in Biological Research: Peptides and Proteins*, North Holland/American Elsevier, New York.
Wüthrich, K. (1986) *NMR of Proteins and Nucleic Acids*, Wiley, New York.
Wüthrich, K. (1989) *Science 243*, 45-50.
Wüthrich, K., Wider, G., Wagner, G., & Braun, W. (1982) *J. Mol. Biol. 155*, 311-319.
Wüthrich, K., Billeter, M., & Braun, W. (1983) *J. Mol. Biol. 169*, 949-961.

NMR Studies of [U-^{13}C]Cyclosporin A Bound to Cyclophilin: Bound Conformation and Portions of Cyclosporin Involved in Binding

S. W. Fesik,* R. T. Gampe, Jr., H. L. Eaton, G. Gemmecker, E. T. Olejniczak, P. Neri, T. F. Holzman, D. A. Egan, R. Edalji, R. Simmer, R. Helfrich, J. Hochlowski, and M. Jackson
Pharmaceutical Discovery Division, Abbott Laboratories, Abbott Park, Illinois 60064
Received January 8, 1991; Revised Manuscript Received April 1, 1991

ABSTRACT: Cyclosporin A (CsA), a potent immunosuppressant, is known to bind with high specificity to cyclophilin (CyP), a 17.7 kDa protein with peptidyl-prolyl isomerase activity. In order to investigate the three-dimensional structure of the CsA/CyP complex, we have applied a variety of multidimensional NMR methods in the study of uniformly ^{13}C-labeled CsA bound to cyclophilin. The ^{1}H and ^{13}C NMR signals of cyclosporin A in the bound state have been assigned, and, from a quantitative interpretation of the 3D NOE data, the bound conformation of CsA has been determined. Three-dimensional structures of CsA calculated from the NOE data by using a distance geometry/simulated annealing protocol were found to be very different from previously determined crystalline and solution conformations of uncomplexed CsA. In addition, from CsA/CyP NOEs, the portions of CsA that interact with cyclophilin were identified. For the most part, those CsA residues with NOEs to cyclophilin were the same residues important for cyclophilin binding and immunosuppressive activity as determined from structure/activity relationships. The structural information derived in this study together with the known structure/activity relationships for CsA analogues may prove useful in the design of improved immunosuppressants. Moreover, the approach that is described for obtaining the structural information is widely applicable to the study of small molecule/large molecule interactions.

Cyclophilin (CyP)[1] is a 17.7 kDa protein (163 residues) that specifically binds to cyclosporin A (CsA; Figure 1), an immunosuppressive drug widely used in organ transplantation (Handschumacher et al., 1984). Although some exceptions have been noted (e.g., MeAla^{6} CsA) (Durette et al., 1988), the relative affinity for cyclophilin within a series of cyclosporin A analogues correlates with their immunosuppressive activities (Handschumacher et al., 1984; Quesniaux et al., 1987, 1988; Durette et al., 1988). Thus, it has been hypothesized that the immunosuppressive activity of CsA is in some way mediated by binding to cyclophilin. The relationship between the binding of cyclosporin A to cyclophilin and the inhibition of T-cell activation at the molecular level is still unresolved. However, it has been suggested that some of the biological effects of CsA (Takahashi et al., 1989) may be linked to the inhibition of the cyclophilin-catalyzed cis-trans isomerization of peptide bonds involving proline (Takahashi et al., 1989; Fischer et al., 1989). As shown for another immunosuppressant (FK506) that binds to a different peptidyl-prolyl cis-trans isomerase, however, isomerase inhibition may not be the only requirement for immunosuppressive activity (Bierer et al., 1990).

In order to aid in the design of CsA analogues that are clinically useful as immunosuppressants, it would be of value to determine the bound conformation of CsA and to identify those portions of CsA that bind to CyP. The CsA analogues synthesized to date (Wenger, 1983, 1985; Durette et al., 1988;

* To whom correspondence should be addressed.

[1] Abbreviations: CyP, cyclophilin; CsA, cyclosporin A; NMR, nuclear magnetic resonance; ATCC, American type culture collection; HMQC, heteronuclear multiple-quantum correlation; TOCSY-REVINEPT, total correlation spectroscopy-reverse insensitive nucleus enhancement by polarization transfer; DIPSI, decoupling in the presence of scalar interactions; GARP, globally optimized alternating-phase rectangular pulses; NOE, nuclear Overhauser effect; COSY, correlation spectroscopy; HMBC, heteronuclear multiple-bond correlation; AMT, American Microwave Technologies; TTL, transistor transistor logic; HSQC, heteronuclear single-quantum correlation; HMQC-NOESY, heteronuclear multiple quantum correlation-nuclear Overhauser effect spectroscopy; TPPI, time-proportional phase incrementation; PTS, programmed test sources; MeAla, *N*-methylalanine; MeVal; *N*-methylvaline; MeBmt, (4*R*)-*N*-methyl-4-butenyl-4-methylthreonine; Abu, aminobutyric acid; Sar, sarcosine; MeLeu, *N*-methylleucine; MePhe, *N*-methylphenylalanine; MeIle, *N*-methylisoleucine; MeThr, *N*-methylthreonine.

0006-2960/91/0430-6574$02.50/0

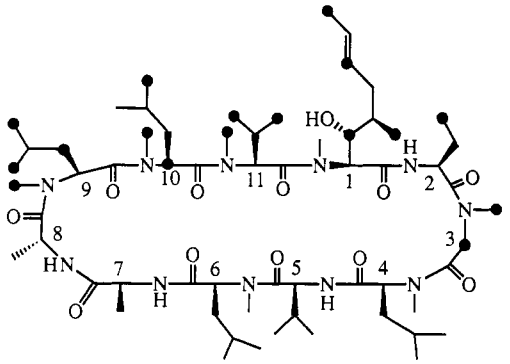

FIGURE 1: Primary structure of cyclosporin A. The filled circles indicate those CsA protons with NOEs to cyclophilin as observed in a 3D HMQC-NOESY experiment acquired with a mixing time of 50 ms.

Aebi et al., 1988, 1990; Rich et al., 1989) have been based on the conformation of CsA determined by X-ray crystallography and NMR spectroscopy in the absence of cyclophilin (Loosli et al., 1985; Lautz et al., 1987). In a recent study (Fesik et al., 1990a) of the CsA/CyP complex using CsA ^{13}C-labeled (>95%) at the 9 and 10 positions, it was shown that CsA adopts a 9,10-trans peptide bond when bound to cyclophilin in contrast to the cis amide bond observed for uncomplexed CsA in solution and in the crystalline state. These studies suggest that the conformation of CsA when bound to cyclophilin is very different from the uncomplexed crystalline and solution conformations of CsA.

In this report we describe our NMR studies of uniformly ^{13}C-labeled CsA bound to recombinant human cyclophilin. From these studies we have assigned the proton and carbon signals of CsA, determined the conformation of CsA when bound to cyclophilin, and identified those portions of CsA that interact with this protein.

Experimental Procedures

Preparation of [U-^{13}C]Cyclosporin A. Spores of *Beauveria nivea* ATCC 34921 (American type culture collection; Rockville, MD) were used to inoculate 500-mL Erlenmeyer flasks containing [U-^{13}C]Celtone medium (Martek Corporation, Columbia, MD) supplemented with 1.2% D-[$^{13}C_6$]glucose (Cambridge Isotope Laboratories, Woburn, MA) in order to obtain [U-^{13}C]CsA (99%). For nonrandomly ^{13}C-labeled CsA, a 3/7 mixture of ^{13}C labeled/unlabeled glucose was part of a minimal medium that contained glucose, 1%; KH_2PO_4, 0.1%; $(NH_4)_2HPO_4$, 0.4%; NaCl, 0.01%; $MgSO_4 \cdot 7H_2O$, 0.05%; $CaCl_2 \cdot 2H_2O$, 0.01%; $FeSO_4 \cdot 7H_2O$, 10 ppm; $ZnSO_4 \cdot 7H_2O$, 8.8 ppm, $CuSO_4 \cdot 5H_2O$, 0.4 ppm; $MnSO_4$, 0.06 ppm; H_3BO_3, 0.06 ppm; and $(NH_4)_6Mo_7O_{24} \cdot 4H_2O$, 0.04 ppm. The flasks were incubated at 28 °C for 6–12 days on a rotary shaker (5.6-cm stroke) at 225 rpm. At harvest, the culture broth (typically 400 mL) was extracted with ethyl acetate (4 × 400 mL). The extracts were combined and concentrated to an oil. This oil was partitioned between methanol (400 mL) and hexane (800 mL), the hexane layer discarded, and the methanol layer concentrated to dryness. This material was triturated with ethyl acetate (400 mL) leaving behind a solid residue. The ethyl acetate soluble material was concentrated to dryness and partitioned between 100 mL each of chloroform, methanol, and distilled water. The lower layer from this partition was concentrated to dryness, then applied to a Sephadex LH-20 column and eluted with a solvent system of heptane/chloroform/ethanol (10:10:1). CsA-containing fractions from this column were combined, concentrated to dryness, and applied to a silica gel column, which was eluted with a gradient of 1–6% methanol in chloroform. From this column was recovered 1.7 mg of pure ^{13}C-labeled CsA. Throughout the isolation, CsA-containing fractions were detected by using the Abbott TD_X instrument with a cyclosporin and metabolites serum reagent pack (Abbott Laboratories, Abbott Park, IL).

Sample Preparation. Recombinant human cyclophilin prepared as recently described (Holzman et al., 1991) was exchanged into a ^2H_2O solution (pH 6.5) containing phosphate buffer (50 mM), NaCl (100 mM), and dithiothreitol (5 mM) and concentrated to 1.3 mM with a centricon YM-10 (Amicon). The [U-^{13}C[CsA/cyclophilin complex was prepared as previously described (Heald et al., 1990) by gently shaking a suspension of ~1.5 mol equivalents of [U-^{13}C]CsA in a D_2O solution of cyclophilin at 6 °C for 12 h under argon. The excess CsA was removed by centrifugation.

NMR. All NMR spectra were acquired on either a Bruker AM500 (500-MHz) or AMX600 (600-MHz) NMR spectrometer at 20 °C. The spectra were processed with in-house written software for Silicon Graphics computers and the Bruker UXNMR software package on a Bruker X32.

The HMQC (Muller, 1979) spectra were collected as previously described (Bax et al., 1983). The 2D ^{13}C TOCSY-REVINEPT spectra (Fesik et al., 1990b) were acquired at 500 MHz with the pulse sequence 90_θ–$t_{1/2}$–$180_x(^1H)$–$t_{1/2}$–DIPSI-2(^{13}C)–τ–$180_x(^1H,^{13}C)$–τ–$90_y(^{13}C),90_\phi(^1H)$–$\tau$–$180_x$-($^1H,^{13}C$)–$\tau$–acquire($t_2$) in which $\theta = X,X,-X,-X$, $\phi = X,-X,X,-X$, and the receiver is cycled $X,-X,-X,X$. DIPSI-2 mixing periods of 8 and 12 ms were used. A BSV3 CW amplifier connected to the observe channel was used for the hard 90° ^{13}C pulses (24 μs) and the DIPSI-2 (Rucker & Shaka, 1985) mixing scheme. An additional BSV3 driven from a PTS synthesizer and interfaced to a GARP box (Tschudin Associates) was used for ^{13}C decoupling during the acquisition period with a GARP decoupling scheme (Shaka et al. 1985). The 2D experiments [$150(t_1) \times 2048(t_2)$] were collected in 16 h each with 128 scans and 4 dummy acquisitions. To enhance the heteronuclear $^{13}C/^1H$ NOE and suppress the residual solvent signal, a series of 90° ^1H pulses separated by 10-ms delays was applied during the delay between scans.

The ^{13}C COSY experiment was collected at 600 MHz in the phase-sensitive mode (Marion et al., 1989) with a sweep width of 31 250 Hz in F_2 and 13 888 Hz in F_1. A total of 288 scans for each of the 128 complex t_1 points were acquired with 8192 complex points in F_2. ^1H decoupling was used during the entire experiment with reduced power during the relaxation delay between scans to avoid excessive sample heating.

The HMBC experiment (Bax & Summers, 1986) was collected at 600 MHz with the pulse sequence $90(^1H)$–τ–90sel(^{13}C=O)–$t_{1/2}$–$180(^1H)$–180sel($^{13}C^\alpha$)–$t_{1/2}$–90sel(^{13}C=O)–t_2 with a delay (τ) of 21 ms. The transmitter frequency for ^{13}C was set to 176.4 ppm, and selective 90° Gaussian pulses (90sel) of 200 μs were used to avoid excitation outside the carbonyl region. Decoupling of the C^α resonances in F_1 was accomplished by applying a selective 180° pulse (180sel) of 300 μs in the middle of the t_1 period. For this purpose, we used an AMT amplifier (gated with a TTL signal from the spectrometer) driven by an external 250-MHz PTS set to a frequency corresponding to a ^{13}C chemical shift of 52 ppm. A total of 32 and 4096 complex points were acquired in t_1 and t_2, respectively. The sweep width was 9434 Hz in F_2 (^1H) and 2841 Hz in F_1 (^{13}C). The data set was processed in mixed mode (Bax & Marion, 1988) with an exponential line broadening (10 Hz) in F_2 and shifted sine bell (45°) in F_1.

The HSQC spectrum (Bodenhausen & Ruben, 1980) was recorded on the AM500 with 4096 real points in F_2 (sequential

acquisition). In F_1, 512 complex points were acquired with 96 scans and 4 dummy scans. The sweep width was 7813 Hz in F_2 and 7463 Hz in F_1.

Several 3D HMQC-NOESY experiments (Fesik & Zuiderweg, 1988) were performed on the AM500 with a variety of mixing times (30, 50, 70, and 140 ms). The NOE data acquired with a mixing time of 50 ms was collected as a series of 47 complex (t_1) 2D experiments [$128(t_2) \times 2048(t_3)$] with a spectral width of 7463 Hz in ω_1 and 7812 Hz in ω_2 and ω_3. A total of 32 acquisitions were collected per t_3 experiment for a total experimental time of approximately 6 days. In order to maintain a steady state and reduce disk I/O, an AM timing accessory (Tschudin Associates) was employed.

The half-filtered 3D HMQC-NOESY experiment was acquired with the pulse sequence $90(^1H)-\Delta-90(^{13}C)-t_{1/2}-180(^1H)-t_{1/2}-90(^{13}C)-\Delta-t_2-90(^1H)-\tau_m-90(^1H)-\Delta-90(^{13}C)-180(^1H)-90(^{13}C)-\Delta-$(acquire)$t_3$ as two separate data sets, one with the last two 90° (^{13}C) pulses with identical phase (i.e., a 180° pulse), the other one with the two pulses with opposite phase (corresponding to a 0° pulse). By adding the two 3D data sets, NOEs from "labeled" CsA protons to other protons attached to ^{13}C-labeled nuclei were removed, leaving only CsA/CyP NOEs. By subtracting the two data sets, only CsA/CsA NOEs remained. Both 3D spectra were acquired on the AM500 with 2048 real points in t_3 (sequential acquisition), 64 complex points in t_2, and 64 complex points in t_1. Sweep widths were 7812.5 Hz in both ^1H dimensions (t_2 and t_3) and 7463 Hz in t_1. Quadrature detection in both indirect dimensions was accomplished according to Marion et al. (1989). For the t_2 incrementation, an external timing device (Tschudin Associates) was used. The residual HDO signal was suppressed by presaturation and irradiation during the 100-ms NOESY mixing delay. ^{13}C composite pulse decoupling was performed with a BSV3 amplifier, driven by an external PTS 250 and modulated by a GARP box (Tschudin Associates). Total measuring time for both experiments was 104 h each. Both data sets were processed separately, after zero filling to 256 complex points in t_2 and 128 complex points in t_1. Linear prediction was used to calculate an additional 16 complex data points in t_2 and t_1 (Olejniczak & Eaton, 1990). The window functions used to process the data were Lorentz-to-Gauss transform (15-Hz line broadening, shift 0.05) in F_3 and Hamming functions shifted by 45° in F_2 and F_1.

The isotope-edited 2D NOE spectrum of a H_2O solution of CsA bound to [U-^{15}N] cyclophilin was collected with the pulse sequence $90(^1H)-t_{1/2}-180(^{15}N)-t_{1/2}-90(^1H)-\tau_m-90(^1H)-\tau-90_\phi(^{15}N)-180_x(^1H)-90_\theta(^{15}N)-\tau-$acquire$(t_2)$ with a phase-cycling scheme for axial peak suppression, quadrature detection (TPPI) in t_1, and suppression of single- and multiple-quantum coherence transfers. In addition, the two 90° ^{15}N pulses were phase cycled: $\phi = X,X$ and $\theta = X,-X$ while maintaining a constant receiver phase (X,X). By use of this half-filter (Otting et al., 1986; Fesik et al., 1987), the signals corresponding to the protons attached to the ^{15}N-labeled nuclei of cyclophilin were removed. The data were acquired at 600 MHz as 215 complex t_1 points (F_1) and 4096 complex points in F_2 with a sweep width of 13 889 Hz in F_2 and 9433 Hz in F_1. A total of 192 scans were acquired for each t_1 value by using a delay $\tau = 5.5$ ms. The large water signal was suppressed by irradiation during the 100-ms mixing time and the relaxation delay between scans. The data was processed with a Lorentz-to-Gauss transform in F_2 (5-Hz line broadening, shifted by 0.15) and a squared sine bell in F_1 (shifted by 60°). A 5th order of polynomial baseline correction was applied in F_2.

Structure Calculations. Three-dimensional structures were calculated by a hybrid distance geometry/dynamical simulated annealing approach (Nilges et al., 1988a; Holak et al., 1989; Clore et al., 1990). DSPACE (Hare Research) was used as the distance geometry algorithm to generate 219 initial structures with the correct chirality after bounds smoothing, embedding into 3D Cartesian space, and conjugate gradient energy minimization. All of these structures were refined by a dynamical simulated annealing protocol (Nilges et al., 1988a,b; Holak et al., 1989; Clore et al., 1990) using the XPLOR program (Brünger, 1990). In stage 1, 50 steps of Powell minimization were applied to ensure a good initial geometry. Stage 2 consisted of 4 ps of molecular dynamics at 1000 K (time step of 2 fs) using the F_{repel} function (Nilges et al., 1988a) for the van der Waals repulsive term with a force constant of 0.002 kcal·mol^{-1}·Å^{-2} and the same radii as in CHARMM (Brooks et al., 1983). NOE constraints were introduced with a soft-square-well potential with an asymptote slope of 0.1 with a value of 0.5 Å for the transition from the square-well to asymptote function. The NOE force constant was 50 kcal·mol^{-1}·Å^{-2}. In stage 3, the asymptote slope was stepwise increased by adding 0.1 to the previous slope to a final value of 1.0. Concomitantly, the van der Waals force constant was increased by multiplying the previous value by 1.5 until a final value of 0.1 was obtained. Each step consisted of 1 ps of restrained molecular dynamics at 1000 K (time step of 2 fs). This stage was followed by slow cooling from 1000 to 300 K in steps of 25 K. During this stage, each step consisted of 0.15 ps restrained molecular dynamics (time step of 2 fs) with a square-well NOE potential, a van der Waals force constant of 4 kcal·mol^{-1}·Å^{-2}, and van der Waals radii of 0.8 times the value used in CHARMM (Brooks et al., 1983) for F_{repel}. In the last stage, the structures were subjected to 500 steps of Powell-restrained energy minimization.

The proton–proton distances, r_{ij}, used as constraints in the structure calculations were obtained from the NOE cross-peak volumes (I_{ij}) measured from a 3D NOE spectrum acquired at a mixing time of 50 ms. The distances were calculated with a known fixed distance of 1.79 Å (distance between α protons of Sar^3) from the equation $r_{ij} \propto I_{ij}^{-1/6}$. A total of 57 proton–proton distances were used in the structure calculations with upper and lower bounds of ± 20% of the calculated distance. For the distances involving methyl groups, 0.5 Å was added to the calculated distance to correct for the pseudoatom. In addition to these constraints, several lower bound constraints were added on the basis of the lack of observable NOEs. These constraints were only included when the absent NOE could be unambiguously interpreted (i.e., no spectral overlap and the observation of other NOEs involving these protons). The minimum approach distance chosen for these constraints was 2.8 Å for NOEs involving single protons and 3.5 Å for NOEs involving methyl groups. NOEs corresponding to these distances were easily observed in the 3D NOE data.

Results and Discussion

Assignments. The NMR signals were assigned (Table I) from an analysis of two-dimensional $^1H/^{13}C$ and $^{13}C/^{13}C$ correlation experiments and NOE data. In the heteronuclear multiple-quantum correlation (HMQC) spectrum (Muller, 1979) shown in Figure 2A, the α, NCH_3, methyl, and some of the MeBmt[1] resonances of CsA were readily identified from their chemical shifts and relative signal intensities. The Sar^3, C^α, and H^α signals were assigned directly from this spectrum, since Sar^3 is the only CsA residue in which two α protons are correlated to the same α carbon.

Table I: ^1H and ^{13}C NMR Assignments of [U-^{13}C]Cyclosporin A Bound to Recombinant Human Cyclophilin

residue	assignment	$^1H^a$	$^{13}C^b$
MeBmt[1]	NCH_3	3.28	34.4
	C=O		172.4
	α	6.82	58.1
	β	4.04	75.7
	γ	1.50	25.0
	δCH3	1.14	15.1
	δ	2.25, 2.60	34.0
	ϵ	5.46	124.3
	ζ	6.15	130.1
	η	1.61	17.2
Abu[2]	NH		
	C=O		172.0
	α	5.02	50.7
	β	1.45, 1.65	24.4
	γ	0.67	9.8
Sar[3]	NCH_3	2.93	33.7
	C=O		170.6
	α	3.04, 5.31	50.9
MeLeu[4]	NCH_3	2.84	29.3
	C=O		171.1
	α	5.15	53.8
	β	1.57, 1.68	36.0
	γ	1.38	23.8
	δ^1	0.93	21.5
	δ^2	0.88	21.8
Val[5]	NH	8.53	
	C=O		174.9
	α	4.30	56.4
	β	2.02	29.4
	γ^1	0.94	18.2
	γ^2	0.93	19.4
MeLeu[6]	NCH_3	3.09	31.8
	C=O		171.9
	α	5.42	54.8
	β	1.73, 1.82	37.0
	γ	1.60	24.0
	δ^1	0.89	22.4
	δ^2	0.78	19.8
Ala[7]	NH	7.56	
	C=O		173.2
	α	4.20	49.3
	β	1.39	17.0
D-Ala[8]	NH	8.33	
	C=O		175.1
	α	4.68	45.3
	β	1.16	15.5
MeLeu[9]	NCH_3	2.61	29.2
	C=O		171.2
	α	5.19	52.1
	β	−0.15, 1.13	36.4
	γ	0.77	22.6
	δ^1	0.32	23.2
	δ^2	0.54	20.2
MeLeu[10]	NCH_3	2.83	32.2
	C=O		173.1
	α	5.98	52.9
	β	1.47, 1.55	36.9
	γ	1.45	25.0
	δ^1	1.10	23.5
	δ^2	1.10	19.1
MeVal[11]	NCH_3	2.73	33.2
	C=O		170.5
	α	4.55	59.3
	β	1.47	24.7
	γ^1	0.47	18.8
	γ^2	−0.69	16.3

[a] ^1H NMR assignments are reported relative to sodium 3-(trimethylsilyl)propionate (0 ppm). [b] ^{13}C NMR assignments are referenced relative to external dioxane (66.5 ppm).

In order to correlate the NMR signals corresponding to the protons and carbons of the individual cyclosporin A spin systems, a 2D ^{13}C TOCSY-REVINEPT experiment (Fesik et al., 1990b) was employed in which a ^{13}C–^{13}C isotropic

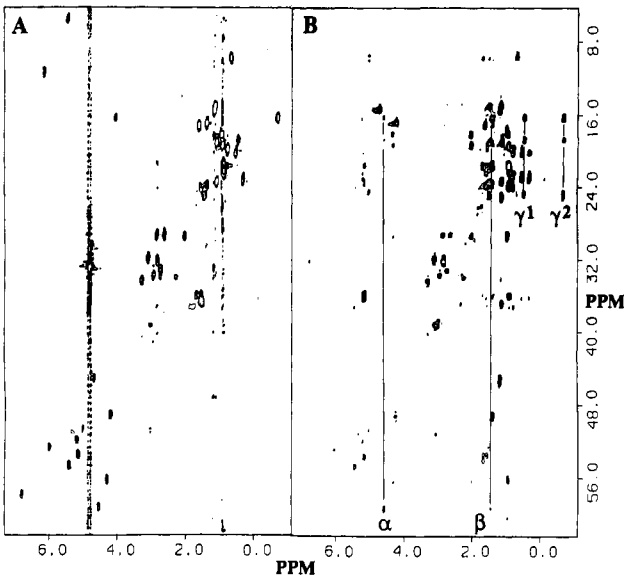

FIGURE 2: (A) $^1H/^{13}C$ heteronuclear multiple-quantum correlation (HMQC) and (B) ^{13}C TOCSY-REVINEPT spectrum (Fesik et al., 1990) of the [U-^{13}C]CsA/cyclophilin complex. Correlations involving the ^{13}C and ^1H spins of MeVal[11] are indicated in the TOCSY–REVINEPT spectrum.

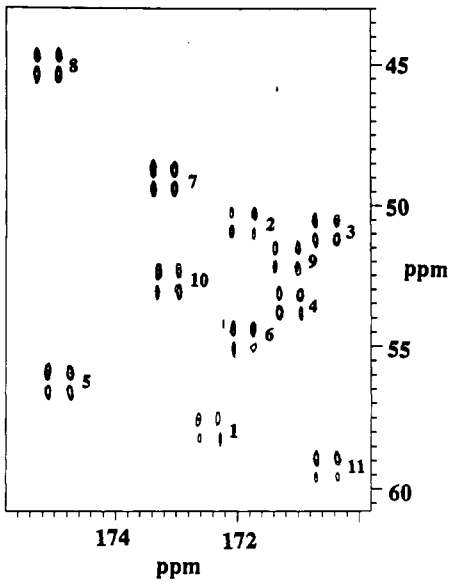

FIGURE 3: Contour plot of a ^{13}C–^{13}C COSY experiment of the [U-^{13}C]CsA/cyclophilin complex. The C=O/C$^\alpha$ correlations are identified in the spectrum by their residue number in CsA.

mixing period was followed by ^{13}C–^1H magnetization transfer. For large molecules, these methods (Fesik et al., 1990b; Kay et al., 1990) are preferred over $^1H/^1H$ correlation experiments for identifying scalar-coupled nuclei, since all of the coherence transfer steps depend on relatively large ^{13}C–^{13}C and ^{13}C–^1H one-bond J-couplings ($^1J_{CC} \geq 35$ Hz and $^1J_{CH} \geq 125$ Hz) and can therefore be effected in a short period of time in this experiment. As illustrated for the MeVal[11] spin system in Figure 2B, the scalar (through-bond) coupled protons and carbons could be identified in the spectrum despite the large size (~19 kDa) of the CsA/cyclophilin complex.

The carbonyl carbons belonging to the individual spin systems were identified in a $^{13}C/^{13}C$ COSY experiment. As shown in Figure 3, all 11 of the expected CsA C=O/C$^\alpha$ cross-peaks were observed in the spectrum.

Sequence-specific assignments of the unique CsA residues (MeBmt[1], Abu[2], and Sar[3]) were obtained directly from the

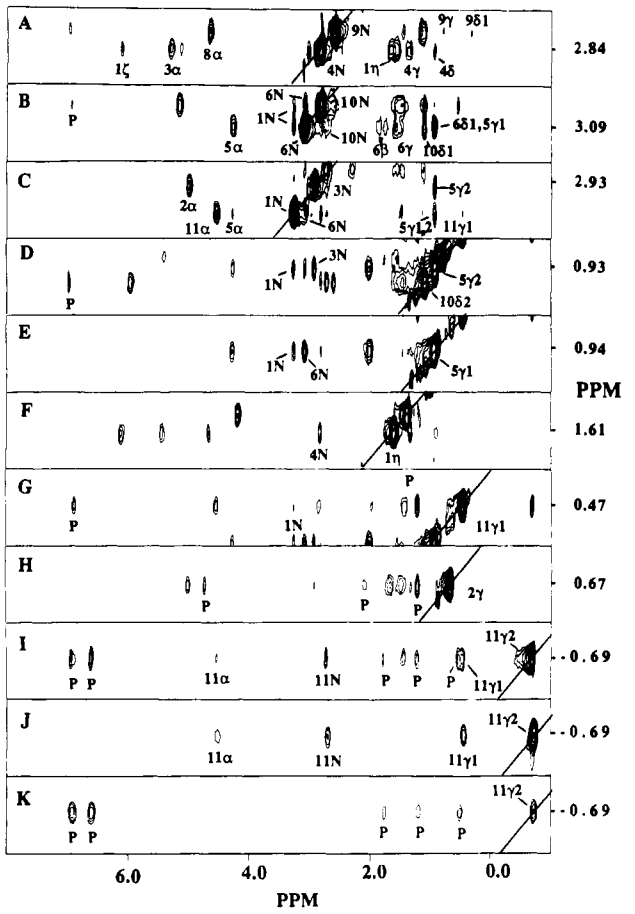

FIGURE 4: (A–I) Cross sections (ω_2, vertical axis; ω_3, horizontal axis) from a 3D ^{13}C HMQC-NOESY data set of the [U-^{13}C]CsA/cyclophilin complex acquired with a mixing time of 50 ms at the ^{13}C chemical shifts (ω_1) (A) 29.3, (B) 31.8, (C) 34.4, (D) 19.4, (E) 18.2, (F) 17.2, (G) 18.8, (H) 9.8, and (I) 16.3 ppm. The diagonal peaks are indicated in each of the planes by a solid line. The NOE cross-peaks occur between protons at the diagonal peak frequencies and other protons along ω_3. The scale for the ω_2 axis is 1.0 ppm. (J, K) Cross sections (ω_2, ω_3) from the half-filtered 3D ^{13}C HMQC-NOESY data set of the [U-^{13}C]CsA bound to cyclophilin at the ^{13}C chemical shift (ω_1) of the γ^2 carbon of MeVal^{11} (16.3 ppm). CsA/CsA NOEs involving the γ^2 protons of MeVal^{11} are present in the subtracted (J) data set, and CsA/CyP NOEs are observed in the added data (K). See cross section I for comparison.

correlation experiments described above. The MeLeu^9 and MeLeu^{10} signals were assigned previously by using a CsA analogue selectively ^{13}C-labeled at residues 9 and 10. The remaining spin systems (D-Ala^8/Ala^7, MeLeu^4/MeLeu^6, and Val^5/MeVal^{11}) were distinguished on the basis of the 3D NOE data (Figure 4) and a heteronuclear multiple-bond correlation (HMBC) experiment (Bax & Summers, 1986) in which the NCH_3 protons and carbonyl carbons of adjacent residues were correlated (Figure 5). The D-Ala^8 and Ala^7 spin systems were distinguished in the HMBC experiment by a correlation between the carbonyl carbon of D-Ala^8 and the NCH_3 protons of MeLeu^9 (previously assigned by using the selectively ^{13}C-labeled CsA analogue). This assignment is consistent with the large MeLeu^9(NCH_3)/D-Ala^8(H^α) NOE observed in a ^{13}C-resolved 3D NOE experiment (Figure 4A). The NCH_3 protons of MeBmt^1, Sar^3, MeLeu^4, and MeLeu^6 were assigned from correlations to the carbonyl carbons of residues 11, 2, 3, and 5, respectively, in the HMBC experiment (Figure 5) and were consistent with the observed $1NCH_3/11H^\alpha$ (Figure 4C), $3NCH_3/2H^\alpha$ (Figure 4C), $4NCH_3/3H^\alpha$ (Figure 4A), and $6NCH_3/5H_\alpha$ (Figure 4B) NOEs. The signals corresponding to the 4- and 6MeLeu residues were distinguished

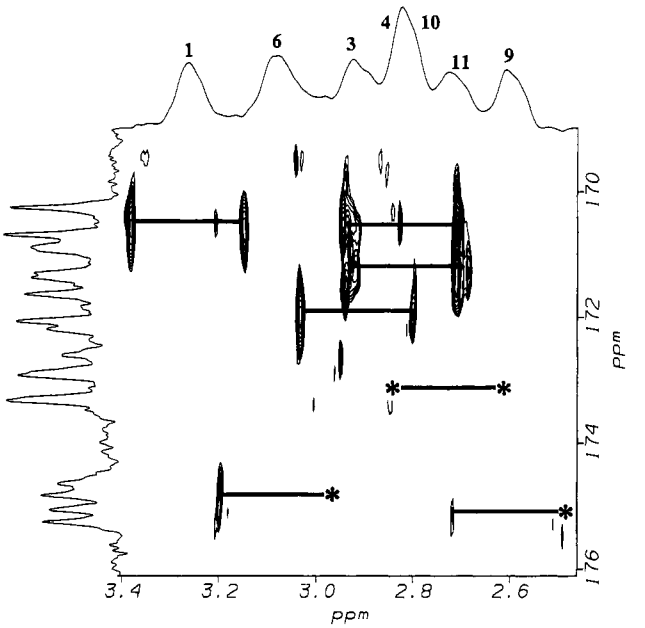

FIGURE 5: Contour plot of an HMBC experiment of the [U-^{13}C]-CsA/cyclophilin complex. In this spectrum, the NCH_3 protons and carbonyl carbons of CsA are correlated. An isotope-edited proton NMR spectrum is shown at the top of the 2D spectrum with the NCH_3 protons labeled. The carbonyl region of a ^{13}C spectrum is depicted to the left of the spectrum. The asterisks denote peaks that could not be observed at this contour level but that were detected at a lower level.

from NOEs between the assigned 4- and $6NCH_3$ protons and their respective side-chain protons (Figure 4A,B). The MeVal^{11} and Val^5 spin systems were distinguished by first assigning the only remaining NCH_3 protons to MeVal^{11} by the NOE between MeVal^{11}(NCH_3) and MeLeu^{10}(H^α), followed by the identification of the other MeVal^{11} signals from MeVal^{11}(NCH_3)/MeVal^{11}(H^β) and MeVal^{11}(NCH_3)/MeVal^{11}-($H^{\gamma 2}$) NOEs.

Three of the four CsA amide protons were assigned from a 2D NOE spectrum of a H_2O solution of CsA bound to [U-^{15}N]cyclophilin in which the signals corresponding to the protons attached to the ^{15}N-labeled nuclei of cyclophilin were removed by a half-filter (Otting et al., 1986; Fesik et al., 1987). As shown in Figure 6, this allowed the observation of the unlabeled amide protons of CsA (as well as other protons of cyclophilin) that resonate in this region of the spectrum. Due to spectral overlap with the aromatic protons of cyclophilin, the Sar^2 amide of CsA could not be unambiguously assigned from the NOE data.

Stereospecific assignments of the γ-methyl groups of Val^5, MeVal^{11}, and the δ-methyl groups of the 4, 6, 9, and 10 MeLeu residues were made from an analysis of a high-resolution heteronuclear single-quantum correlation (HSQC) spectrum (Bodenhausen & Ruben, 1980) of a CsA/CyP complex composed of ^{13}C-labeled CsA prepared biosynthetically from a 3/7 mixture of uniformly ^{13}C-labeled and unlabeled glucose. During the biosynthesis of valine and leucine (Sylvester & Stevens, 1979; Crout et al., 1980), the isopropyl group is derived from a two-carbon fragment containing the pro-*R* methyl and a migrating methyl group (pro-*S*) originating from a different pyruvate. As previously demonstrated by Wüthrich and co-workers (Senn et al., 1989; Neri et al., 1989, 1990), the stereoselective biosynthetic reactions allow the pro-*S* and pro-*R* methyl groups to be distinguished. The ^{13}C NMR signal of the pro-*R* methyl groups of valine (γ^1) and leucine (δ^1) are coupled (J = 35 Hz) to the β and γ carbons, respectively,

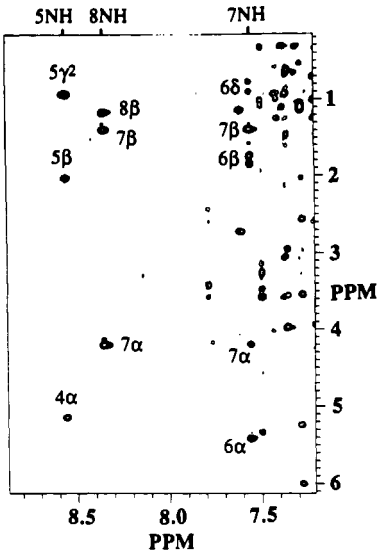

FIGURE 6: Contour plot of an isotope-edited 2D NOE spectrum of a 1.3 mM solution of CsA and [U-^{15}N] human cyclophilin (1:1) in H_2O in which the signals corresponding to the protons attached to the ^{15}N-labeled nuclei of cyclophilin were removed by a half-filter (Otting et al., 1986; Fesik et al., 1987). Three of the four unlabeled amide protons of CsA (as well as other protons of cyclophilin) are observed in this region of the spectrum. The CsA amides (top) and NOEs involving these protons are indicated in the spectrum.

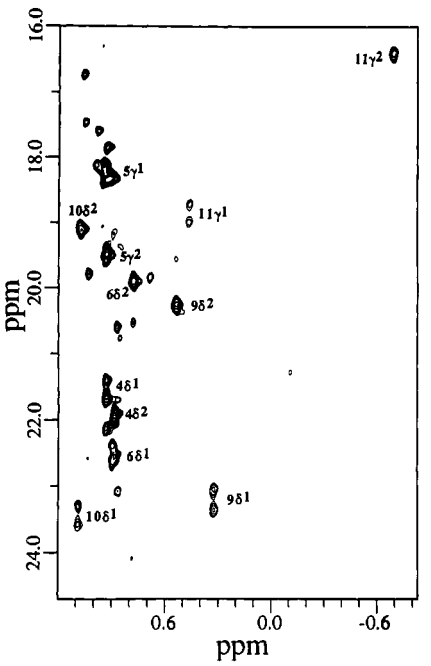

FIGURE 7: Portion of a 2D HSQC spectrum of the nonrandomly ^{13}C-labeled (30%) CsA bound to cyclophilin. The pro-*R* (γ^1, δ^1) and pro-*S* (γ^2, δ^2) methyl signals of CsA residues determined by the ^{13}C–^{13}C coupling pattern are indicated.

whereas the pro-*S* methyls (γ^2, δ^2) appear as a singlet (at this level of enrichment a doublet of 4-fold less signal intensity is observed superimposed on the singlet). Compared to previous studies (Senn et al., 1989; Neri et al., 1989, 1990) in which a relatively low amount of ^{13}C enrichment was employed, a higher level of ^{13}C labeling was used in this study to reduce the amount of background from the signals corresponding to cyclophilin at natural abundance. As shown in Figure 7, the background protein signals did not interfere significantly with the identification of the CsA resonances, and the stereospecific assignments were readily obtained from the spectrum.

Bound Conformation of CsA. In the ^{13}C-resolved 3D NOE spectrum, NOEs were observed that originated from protons attached to the ^{13}C-labeled nuclei of CsA to other protons of CsA and cyclophilin. By editing in a third dimension by the ^{13}C frequencies in the 3D NMR experiment, many NOEs were well-resolved and easily assigned. For example, as illustrated in Figures 4D and 4E, the NOEs involving $H^{\gamma 2}$ and $H^{\gamma 1}$ of Val^5 that resonate at nearly the same frequency are clearly distinguished in a ^{13}C-resolved 3D NOE experiment at their different ^{13}C frequencies. CsA/CsA and CsA/CyP NOEs were distinguished from one another by the presence or absence of diagonally related peaks. CsA/CsA NOEs were detected from both NOE partners at the two corresponding ^{13}C frequencies [e.g., Sar^3(NCH$_3$)/Val^5($H^{\gamma 2}$), (Figure 4C) and Val^5($H^{\gamma 2}$)/Sar^3(NCH$_3$), (Figure 4D)], whereas CsA/cyclophilin NOEs were only detected in one plane at the CsA ^{13}C frequencies. These NOEs were also distinguished in a F_3 half-filtered 3D NOE experiment by combining two 3D NOE data sets that were acquired with or without at 180° carbon pulse during the half-filter. This experiment is analogous to previously described double half-filtered 2D experiments (Otting & Wüthrich, 1989; Wider et al., 1990) with the advantage of improved resolution offered by the third dimension. In the difference of the two 3D data sets, only CsA/CsA NOEs were observed, and in the added data only CsA/cyclophilin NOEs were detected. For example, the CsA/CsA and CsA/CyP NOEs arising from MeVal^{11}($H^{\gamma 2}$) in the 3D NOE spectrum (Figure 4I) were unambiguously distinguished in the subtracted (Figure 4J) and added (Figure 4K) half-filtered 3D NOE spectrum.

For a qualitative interpretation of the 3D NOE data, NOE cross-peaks were analyzed from the different ^{1}H–^{1}H 2D planes at the individual ^{13}C frequencies. However, the magnitude of the NOE peaks was difficult to determine from a simple analysis of the 2D planes, since the cross-peaks intensity was spread over more than one plane, depending in part on the ^{13}C line width and ^{13}C–^{13}C coupling pattern. Therefore, in order to obtain a semiquantitative interpretation of the 3D NOE data, the 3D NOE cross-peak volumes were used. From the integrated 3D NOE cross-peak volumes measured from a 3D NOE data set acquired with a mixing time of 50 ms and a known proton–proton distance, unknown proton–proton distances were estimated. The upper and lower bounds (±20% of the calculated distance) used in the structure calculations were rather conservative due to the potential error in the calculated distances from spin diffusion effects and differences in the relaxation properties of the nuclei. Indeed, spin diffusion effects were clearly evident between the β protons of MeLeu residues even in the 50-ms NOE data. Thus, the additional 32 NOEs that were observed involving the β protons were not included in the structure calculations as distance constraints due to the large errors associated with these distances. All of the 32 additional NOEs were intraresidue NOEs within MeLeu residues. For these constraints, spin diffusion effects must be taken into account, and the distances involving these protons must be accurately calculated (e.g., by using a method that includes a full relaxation rate matrix) (Olejniczak et al., 1986). These studies are in progress.

The fixed distance used in the calculations was the distance between the two α protons of Sar^3. Other known distances calculated from the NOE data (e.g., $H\beta^2/H\beta^2$ of MeLeu^9 and Abu^2) were all within 0.1 Å of the actual distance. A total of 219 initial structures were generated from the DSPACE distance geometry algorithm and further refined with dynamical simulated annealing using XPLOR (Brünger, 1988). From these structures, 95 were chosen that best satisfied the

FIGURE 8: Stereoview of the superposition of the 20 CsA structures with the lowest NOE energy contribution out of 95 converged structures.

Table II: Structural Statistics and Atomic rms Differences[a]

	Structural Statistics		
	⟨SA⟩	$\overline{SA}$	$(\overline{SA})_m$
rms deviation from distance constraints (Å)[b]	0.023 ± 0.002	0.017	0.031
E_{NOE} (kcal/mol)[c]	1.935 ± 0.323	0.996	3.591
E_{repel} (kcal/mol)[d]	3.695 ± 0.369	217.17	7.792
E_{L-J} (kcal/mol)[e]	−15.25 ± 2.89	10070	−8.61
deviation from idealized geometry			
bonds (Å)	0.010 ± 0.0005	0.451	0.012
angles (deg)	2.242 ± 0.033	47.859	2.668
impropers (deg)	0.178 ± 0.012	0.304	0.303

	Atomic rms Differences	
	backbone (C',N,C$^\alpha$)	all heavy atoms
⟨SA⟩ vs $\overline{SA}$	0.37 ± 0.11	0.50 ± 0.14
⟨SA⟩ vs $(\overline{SA})_m$	0.69 ± 0.08	0.95 ± 0.10
$\overline{SA}$ vs $(\overline{SA})_m$	0.77	0.81

[a] ⟨SA⟩ refers to the average value over the final 95 structures; $\overline{SA}$ refers to the average structure; $(\overline{SA})_m$ refers to the structure obtained after restrained energy minimization of SA. [b] None of the structures violated the constraints greater than 0.2 Å. [c] E_{NOE} is the energy contribution from the square-well NOE potential using a force constant of 50 kcal·mol^{-1}·Å^{-2}. [d] E_{repel} is the van der Waals repulsion energy term calculated with the F_{repel} potential (Nilges et al., 1988a) and a force constant of 4 kcal·mol^{-1}·Å^{-2} and a hard-sphere van der Waals radii 0.8 times the CHARMM (Brooks et al., 1983) function. [e] E_{L-J} is the Lennard-Jones van der Waals energy calculated by using the CHARMM function.

experimentally derived distance constraints. All of these structures satisfied every distance constraint to within 0.2 Å. Furthermore, as shown in Table II, the structures have relatively minor deviations from idealized geometry. For these 95 structures, the average rms deviation of the backbone atoms to a calculated average structure was 0.37 (±0.11) Å and for all of the heavy atoms was 0.50 (±0.14) Å. A total of 20 CsA structures with the lowest NOE energy contribution were chosen from the final 95 structures and are depicted in Figure 8.

CsA was found to adopt an extended backbone conformation in which all of the peptide bonds are trans. This is supported by the lack of NOEs between α protons of adjacent residues, which would be indicative of cis peptide bonds, the large $NCH_3(i+1)/H^\alpha(i)$ (Figure 4A–C) or $NH(i+1)/H^\alpha(i)$ NOEs (Figure 6), and, with the exception of MeLeu^4 and Ala^7, the weak intraresidue NCH_3/H^α and NH/H^α NOEs. The NOE data support a conformation in which residues 9, 11, 2 and 4, 6 are located on opposite sides of the macrocyclic ring with their side chains pointing outward away from the macrocyclic ring. The side chains of residues 10, 1, and 5, on the other hand, face inward toward the center of the ring. Some of the specific long-range NOEs that support this conformation include MeBmt^1(NCH_3)/Val^5($H^{\gamma 1}$) (Figure 4C,E); MeBmt^1-(NCH_3)/Val^5($H^{\gamma 2}$) (Figure 4C,D); MeLeu^6(NCH_3)/MeLeu^{10}($H^{\delta 1}$) (Figure 4B); Sar^3(NCH_3)/Val^5($H^{\gamma 2}$) (Figure 4C,D); MeLeu^4(NCH_3)/MeBmt^1(H^η) (Figure 4A,F); MeLeu^6(NCH_3)/MeBmt^1(NCH_3) (Figure 4B,C); MeBmt^1-(NCH_3)/MeLeu^{10}(NCH_3) (Figure 4B,C); and MeLeu^6-(NCH_3)/MeLeu^{10}(NCH_3) (Figure 4B).

The side-chain conformations of Val^5 and MeVal^{11} were also determined from the 3D NOE data. Both residues contain a χ_1 angle of ~180°, which is supported by very small H^α/H^β NOEs, NOEs of equal intensity between H^α, and $H^{\gamma 1}$, and $H^{\gamma 2}$, and by MeBmt^1(NCH_3)/MeVal^{11}($H^{\gamma 1}$) (Figure 4C,G), MeVal^{11}(NCH_3)/MeVal^{11}($H^{\gamma 2}$) (Figure 4I), MeLeu^6-(NCH_3)/Val^5($H^{\gamma 1}$) (Figure 4B,E), and Val^5(NH)/Val^5($H^{\gamma 2}$) (Figure 5) NOEs. For all of the MeLeu residues a χ_1 of ~−60° is supported by intraresidue NCH_3/H^γ NOEs (Figure 4A,B). The χ_2 angle for residues 6, 9, and 10 was found to be ~180° on the basis of the strong intraresidue $H^\alpha/H^{\delta 2}$ NOE for each of these residues. The side-chain conformation of MeLeu^4 could not be determined unambiguously.

It was of interest to compare the cyclophilin-bound conformation of CsA to the three-dimensional structure of CsA that had been previously determined by X-ray crystallography and NMR in the absence of cyclophilin (Loosli et al., 1985). When bound to cyclophilin, CsA adopts a 9,10-trans peptide bond (Fesik et al., 1990a) in contrast to the 9,10-cis peptide bond found in the previously determined structures (Loosli et al., 1985). In addition, the NCH_3 protons of residues 1, 6, and 10 are close to one another in the bound conformation but are far apart in the crystal structure (Loosli et al., 1985), suggesting marked differences in the backbone conformation (Figure 9). The orientations of some of the side chains also differ between the structures. When CsA is bound to cyclophilin, the Val^5 side chain points toward the ring (Figure 9) and is near the NCH_3 group of Sar^3. In contrast, in the crystal and solution structure of CsA determined in the absence of cyclophilin (Loosli et al., 1985), the Val^5 side chain is pointing away from the ring and is closer to the NCH_3 group of MeLeu^4. The location of the MeLeu^{10} side chain of CsA was also found to be different in the structures. When bound to cyclophilin, the MeLeu^{10} side chain points toward the ring and is near the NCH_3 protons of MeLeu^6, whereas, in the crystal structure (Loosli et al., 1985), the MeLeu^{10} side chain points

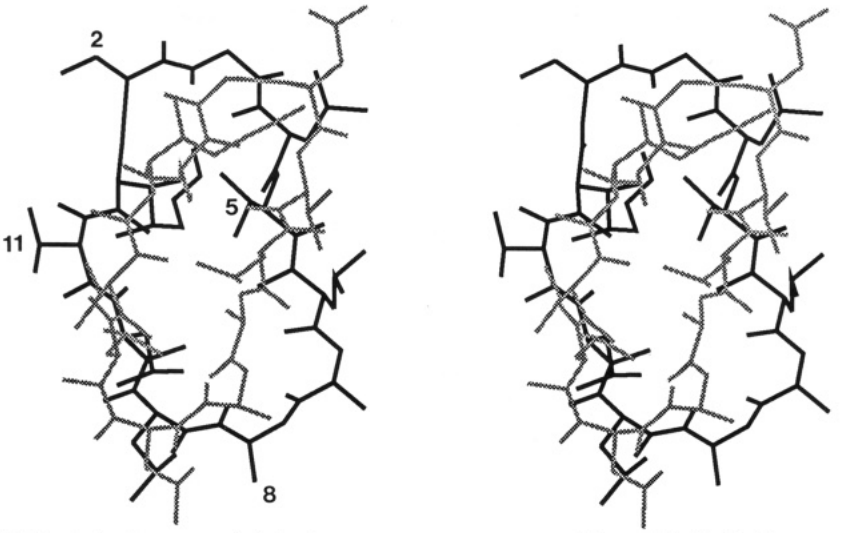

FIGURE 9: Stereoview of CsA (restrained energy-minimized average structure generated from 95 individual structures) bound to cyclophilin (black) superimposed on the X-ray crystal structure of CsA (grey) (Loosli et al., 1985) determined in the absence of cyclophilin.

away from the ring and is far apart from MeLeu^6(NCH_3). The MeBmt^1 side chain is folded back across the ring either in the crystal structure or in solution when bound to cyclophilin but is located on opposite faces with respect to the main plane of the CsA ring. Moreover, its exact location in the two structures differs as evidenced by the MeBmt^1(H^η)/MeLeu^4(NCH_3) (Figure 4A,F) and MeBmt^1(H^δ)/MeLeu^4(NCH_3) (Figure 4A) NOEs. In the crystal structure (Loosli et al., 1985), these protons are far apart.

Portions of Cyclosporin A in Close Proximity to Cyclophilin. NOEs between cyclosporin A and cyclophilin were used to identify those portions of CsA that interact with the protein. Figure 1 schematically depicts the CsA protons that are in close proximity to cyclophilin as evidenced by CsA/CyP NOEs observed in a 3D NOE spectrum acquired with a mixing time of 50 ms. NOEs were observed between the protons of the MeLeu^9 residue and aromatic protons of cyclophilin that were tentatively assigned (Fesik et al., 1990a) to Trp^{121} and Phe protons. The MeLeu^{10}(NCH_3) (Figure 4B), MeLeu^{10}($H^{\delta 2}$) (Figure 4D), MeLeu^{10}(H^α), MeVal^{11}(NCH_3), MeVal^{11}($H^{\gamma 1}$) (Figure 4G), MeVal^{11}($H^{\gamma 2}$) (Figure 4I,K), MeBmt^1(H^β),MeBmt^1(H^δ), MeBmt^1(H^ϵ), and MeBmt^1(H^η) protons of CsA are also all near aromatic (as well as aliphatic) protons of cyclophilin. The Sar^3($H^{\alpha 1}$), Sar^3($H^{\alpha 2}$), and Abu^2(H^γ) (Figure 2H) protons of CsA are not close to aromatic but only to aliphatic protons of cyclophilin. Additional CsA/CyP NOEs were observed in the 3D NOE spectra acquired with longer mixing times (e.g., 140 ms) that were not detected in the NOE data with a 50-ms mixing time. Some of these NOEs were interpreted as peaks arising from spin diffusion and were therefore not included in Figure 1.

The CsA/CyP NOEs that were observed are consistent with the bound conformation of CsA. For example, the MeVal^{11} NCH_3 and $H^{\gamma 1}$ protons of CsA, which are close to one another, both have NOEs to cyclophilin protons that resonate at 6.96, 6.64, and 0.93 ppm. NOEs were also observed between the MeVal^{11}($H^{\gamma 1}$) and Abu^2(H^γ) protons of CsA and cyclophilin protons that resonate at 4.73 and 1.21 ppm. Although no NOE was observed between the MeVal^{11}($H^{\gamma 1}$) and Abu^2(H^γ) protons of CsA, the side chains of CsA residues 11 and 2 both point in the same direction away from the CsA ring in a location that could explain the observed NOEs.

As a general rule, those portions of CsA that were found to be close to cyclophilin as evidenced by CsA/cyclophilin NOEs were those CsA residues important for cyclophilin binding (Handschumacher et al., 1984; Quesniaux et al., 1987, 1988; Durette et al., 1988) and immunosuppressive activity (Wenger 1983, 1985; Durette et al., 1988; Aebi et al., 1988, 1990; Rich et al., 1989) as determined from structure/activity relationships. Cyclophilin binding affinity and immunosuppressive activity is particularly sensitive to most modifications at either the MeVal^{11} or MeBmt^1 CsA residues as evidenced by a dramatic loss of activity for MeAla^{11}, MeLeu^{11}, MeIle^{11}, (OAc)MeBmt^1, (3′-deoxy)MeBmt^1, and MeThr^1 CsA analogues (Wenger, 1983, 1985; Durette et al., 1988; Quesniaux, et al., 1987). Indeed, both 1 and 11 CsA residues are close to cyclophilin on the basis of NOEs observed between these residues and cyclophilin. Similarly, CsA analogues modified at the MeLeu^{10} position (e.g., MeAla^{10} and MePhe^{10} CsA) do not bind as well to cyclophilin and are less potent immunosuppressants (Durette et al., 1988; Quesniaux, et al., 1987), consistent with the NOEs observed between the MeLeu^{10} protons of CsA and cyclophilin.

The Abu^2 residue of cyclosporin appears to be less sensitive to modifications than some of the other CsA residues. CsA derivatives containing Thr^2 (CsC), NorVal^2 (CsG), Ala^2, Val^2, and fluorinated amino acids were all biologically active (Wenger, 1983, 1985; Durette et al., 1988; Quesniaux, et al., 1987). However, analogues containing much larger substituents at the 2 position were less potent (Quesniaux et al., 1987), suggesting a limited amount of space due to the close proximity of cyclophilin to the Abu^2 residue of CsA. This is consistent with the NOEs observed between the Abu^2 methyl protons of CsA and cyclophilin.

It has been suggested (Quesniaux et al., 1987) that all of the other CsA residues (3, 4, 5, 6, 7, 8, and 9) have no significant interaction with cyclophilin. In contrast, other workers (Durette et al., 1988) have concluded on the basis of MeAla- and Ala-substituted CsA analogues that residues 4, 5, and 9 of CsA are important for binding to cyclophilin and immunosuppressive activity. The NOE data clearly indicate that the MeLeu^9 residue of CsA is interacting with aromatic amino acid residues of cyclophilin. However, in contrast to the conclusions of Durette et al. (1988), the side chains of CsA residues 4 and 5 do not appear to be in close proximity to cyclophilin on the basis of the NOEs.

Although several CsA derivatives containing modifications at residue 3 still retain significant biological activity (e.g., D-MeAla^3 and D-MePhe^3 CsA) (Durette et al., 1988; Quesniaux et al., 1987; Aebi et al., 1988), other CsA analogues

containing a L-MeAla or D-Pro at the 3 position are inactive (Wenger, 1983, 1985; Aebi et al., 1988). The loss of activity displayed by L-MeAla[3] CsA was suggested (Aebi et al., 1988) to be due to the inability of this analogue to adopt a 3,4 type II′ β-turn as found in the crystalline and solution conformation of CsA determined in the absence of cyclophilin (Loosli et al., 1985). Conversely, the loss of activity of the D-Pro[3] CsA analogue was attributed (Aebi et al., 1988) to steric hindrance with the cyclosporin receptor. The NOE observed between the Sar[3] α protons of CsA and cyclophilin suggests that this residue is close to cyclophilin. Therefore, bulky substituents at the 3 position could prevent a favorable interaction with the protein. However, for some analogues, the inability to adopt the cyclophilin-bound CsA conformation could also be a contributing factor.

In all studies on structure/activity relationships, the Ala[7] and D-Ala[8] residues of CsA have been shown to be relatively unimportant for immunosuppressive activity and cyclophilin binding. Indeed, the D-Lys[8] CsA analogue with the side chain of D-Lys[8] covalently attached to a column support has been used as an affinity column to purify cyclophilin (Quesniaux et al., 1987). These results are consistent with the lack of NOEs observed between these residues and cyclophilin.

For the 6 position, MeAla[6] and NorVal[6] CsA appear to bind quite well to cyclophilin (~50% binding affinity compared to CsA), whereas MeVal[6], MeIle[6], and MePhe[6] CsA bind only weakly to cyclophilin (Durette et al., 1988). The lack of NOEs observed between the side chain of residue 6 and cyclophilin suggests that the reduced activity for some of these analogues may not be due to an unfavorable interaction with cyclophilin but may arise from conformational differences. In order to test this hypothesis, it would be of interest to determine the conformation of the β-branched 6-position CsA analogues when bound to cyclophilin. It would also be of interest to study the MeAla[6] CsA when bound to cyclophilin, since unlike other CsA analogues, the relative cyclophilin binding affinity of MeAla[6] CsA does not correlate with its immunosuppressive activity (Durette et al., 1988).

Conclusions

Through the use of a ^{13}C-labeled ligand and a variety of heteronuclear two- and three-dimensional NMR techniques, we have assigned the ^{1}H and ^{13}C NMR signals and determined the conformation of a ligand when bound to its putative target protein. In addition, we have identified those portions of the ligand that are close to the protein-binding site. These results and those derived independently by Wüthrich and co-workers (Weber et al., 1991), illustrate the utility of this approach for obtaining detailed structural information from NMR data on a protein/ligand complex of moderate size. The structural information derived from such an approach could potentially be used to aid in the design of analogues that have greater clinical utility than the lead compound. From the structural information derived in this study, CsA analogues could be designed that are structurally very dissimilar to the parent molecule and yet have the important functional groups in their proper orientation for binding to cyclophilin. These analogues (which would be difficult to design in the absence of 3D structural information) may have improved physical properties and less toxic side effects, making them more suitable as immunosuppressive agents.

Acknowledgments

We thank G. W. Carter, J. Luly, R. Pariza, J. McAlpine, and T. J. Perun for their support and encouragement and Erik Zuiderweg for critical reading of the manuscript. H.L.E. is supported as a postdoctoral associate in part by NIH Grant U01 AI27220-01, and P.N. acknowledges support from a fellowship from the CNR, Italy (bando no. 203.03.22, Com. Scienze Chimiche).

References

Aebi, J. D., Guillaume, D., Dunlap, B. E., & Rich, D. H. (1988) *J. Med. Chem. 31*, 1805.

Aebi, J. D., Deyo, D. T., Sun, C. Q., Guillaume, D., Dunlap, B., & Rich, D. H. (1990) *J. Med. Chem. 33*, 999.

Bax, A., & Summers, M. F. (1986) *J. Am. Chem. Soc. 108*, 2093.

Bax, A., & Weiss, M. A. (1987) *J. Magn. Reson. 71*, 571.

Bax, A., & Marion, D. (1988) *J. Magn. Reson. 78*, 186.

Bax, A., Griffey, R. H., & Hawkins, B. L. (1983) *J. Magn. Reson. 55*, 301.

Bierer, B. E., Somers, P. K., Wandless, T. J., Burakoff, S. J., & Schreiber, S. L. (1990) *Science 250*, 556.

Bodenhausen, G., & Ruben, D. J. (1980) *Chem. Phys. Lett. 69*, 185.

Brooks, B. R., Bruccoleri, R. E., Olfason, B. D., States, D. J., Swaminathan, S., & Karplus, M. (1983) *J. Comput. Chem. 4*, 187.

Brünger, A. T. (1990) XPLOR Manual, version 2.1.

Clore, G. M., Apella, E., Yamada, M., Matsushima, K., & Gronenborn, A. M. (1990) *Biochemistry 29*, 1689.

Crout, D. H. G., Hedgecock, J. R., Lipscomb, E. L., & Armstrong, F. B. (1980) *J. Chem. Soc., Chem. Commun.*, 304.

Durette, P. L., Boger, J., Dumont, F., Firestone, R., Frankshun, R. A., Koprak, S. L., Lin, C. S., Melino, M. R., Pessolano, A. A., Pisano, J., Schmidt, J. A., Sigal, N. H., Staruch, M. J., & Witzel, B. E. (1988) *Transplant. Proc. 20*, 51.

Fesik, S. W., & Zuiderweg, E. R. P. (1988) *J. Magn. Reson. 78*, 588.

Fesik, S. W., Gampe, R. T., Jr., & Rockway, T. W. (1987) *J. Magn. Reson. 74*, 366.

Fesik, S. W., Luly, J. R., Erickson, J. W., & Abad-Zapatero, C. (1988) *Biochemistry 27*, 8297.

Fesik, S. W., Gampe, R. T., Jr., Holzman, T. F., Egan, D. A., Edalji, R., Luly, J. R., Simmer, R., Helfrich, R., Kishore, V., & Rich, D. H. (1990a) *Science 250*, 1406.

Fesik, S. W., Eaton, H. L., Olejniczak, E. T., & Zuiderweg, E. R. P. (1990b) *J. Am. Chem. Soc. 112*, 886.

Fischer, G., Wittman-Liebold, B., Lang, K., Kiefhaber, T., & Schmid, F. X. (1989) *Nature 337*, 476.

Handschumacher, R. E., Hardin, M. W., Rice, J., Drugge, R. J., & Speicher, D. W. (1984) *Science 226*, 544.

Heald, S. L., Harding, M. W., Handschumacher, R. E., & Armitage, I. M. (1990) *Biochemistry 29*, 4466.

Holak, T. A., Gondol, D., Otlewski, J., & Wilusz, T. (1989) *J. Mol. Biol. 210*, 635.

Holzman, T. F., Egan, D. A., Edalji, R., Simmer, R. S., Helfrich, R., Taylor, A., & Burres, N. S. (1991) *J. Biol. Chem. 266*, 2474.

Kay, L. E., Ikura, M., & Bax, A. (1990) *J. Am. Chem. Soc. 112*, 888.

Lautz, J., Kessler, H., Kaptein, R., & van Gunsteren, W. F. (1987) *J. Comput. Aided Mol. Des. 1*, 219.

Loosli, H. R., Kessler, H., Oschkinat, H., Weber, H.-P., Petcher, T. J., & Widmer, T. J. (1985) *Helv. Chim. Acta 68*, 682.

Marion, D., Ikura, M., Tschudin, R., & Bax, A. (1989) *J. Magn. Reson. 85*, 393.

Muller, L. (1979) *J. Am. Chem. Soc. 101*, 4481.
Neri, D., Szyperski, T., Otting, G., Senn, H., & Wüthrich, K. (1989) *Biochemistry 28*, 7510.
Neri, D., Otting, G., & Wüthrich, K. (1990) *Tetrahedron 46*, 3287.
Nilges, M., Clore, G. M., & Gronenborn, A. M. (1988a) *FEBS Lett. 229*, 317.
Nilges, M., Clore, G. M., & Gronenborn, A. M. (1988b) *FEBS Lett. 239*, 129.
Olejniczak, E. T., & Eaton, H. L. (1990) *J. Magn. Reson. 87*, 628.
Olejniczak, E. T., Gampe, R. T. Jr., & Fesik, S. W. (1986) *J. Magn. Reson. 67*, 28.
Otting, G., & Wüthrich, K. (1989) *J. Magn. Reson. 85*, 586.
Otting, G., Senn, H., Wagner, G., & Wüthrich, K. (1986) *J. Magn. Reson. 70*, 500.
Quesniaux, V. F. J., Schreier, M. H., Wenger, R. M., Hiestand, P. C., Harding, M. W., & Van Regenmortel, M. H. V. (1987) *Eur. J. Immunol. 17*, 1359.
Quesniaux, V. F. J., Schreier, M. H., Wenger, R. M., Hiestand, P. C., Harding, M. W., & Van Regenmortel, M. H. V. (1988) *Transplantation 46*, 23S.
Rich, D. H., Sun, C.-Q., Guillaume, D., Dunlap, B., Evans, D. A., & Weber, A. (1989) *J. Med. Chem. 32*, 1982.
Rucker, S. P., & Shaka, A. J. (1989) *Mol. Phys. 68*, 509.
Senn, H., Werner, B., Messerle, B., Weber, C., Traber, R., & Wüthrich, K. (1989) *FEBS Lett. 249*, 113.
Shaka, A. J., Barker, P. B., & Feeman, R. (1985) *J. Magn. Reson. 64*, 547.
Sylvester, S. R., & Stevens, C. M. (1979) *Biochemistry 18*, 4529.
Takahashi, N., Hayano, T., & Suzuki, M. (1989) *Nature 337*, 473.
Weber, C., Wider, G., von Freyberg, B., Traber, R., Braun, W., Widmer, H., & Wüthrich, K. (1991) *Biochemistry*, preceding paper in this issue.
Wenger, R. (1983) *Transplant. Proc. 15*, 2230.
Wenger, R. M. (1985) *Angew. Chem. Int. Ed. Engl. 24*, 77.
Wider, G., Weber, C., Traber, R., Widmer, H., & Wüthrich, K. (1990) *J. Am. Chem. Soc. 112*, 9015.

Dynamics of the Quaternary Conformational Change in Trout Hemoglobin

James Hofrichter,* Eric R. Henry, Attila Szabo, Lionel P. Murray,‡ Anjum Ansari, Colleen M. Jones, Massimo Coletta,§ Giancarlo Falcioni,§ Maurizio Brunori,§,∥ and William A. Eaton

Laboratory of Chemical Physics, National Institute of Diabetes and Digestive and Kidney Diseases, National Institutes of Health, Bethesda, Maryland 20892

Received August 23, 1990; Revised Manuscript Received January 31, 1991

ABSTRACT: The kinetics of conformational changes in trout hemoglobin I have been characterized over the temperature range 2–65 °C from time-resolved absorption spectra measured following photodissociation of the carbon monoxide complex. Changes in the spectra of the deoxyheme photoproduct were used to monitor changes in the protein conformation. Although the deoxyheme spectral changes are only about 8% of the total spectral change due to ligand rebinding, a combination of high-precision measurements and singular value decomposition of the data permits a detailed analysis of both their amplitudes and relaxation rates. Systematic variation of the degree of photolysis was used to alter the distribution of liganded tetramers, permitting the assignment of the spectral relaxation at 20 μs to the R → T quaternary conformational change of the zero-liganded and singly liganded molecules and spectral relaxations at about 50 ns and 2 μs to tertiary conformational changes within the R structure. Analysis of the effect of photoselection by the linearly polarized excitation pulse indicates that a major contribution to the apparent geminate rebinding in the 50-ns relaxation arises from rotational diffusion of molecules containing unphotolyzed heme–CO complexes. The activation enthalpy and activation entropy for the $R_0 \rightarrow T_0$ transition are +7.4 kcal/mol and −12 cal mol^{-1} K^{-1}. Using the equilibrium data, ΔH = +29.4 kcal/mol and ΔS = +84.4 cal mol^{-1} K^{-1} [Barisas, B. G., & Gill, S. J. (1979) *Biophys. Chem. 9*, 235–244], the activation parameters for the $T_0 \rightarrow R_0$ transition are calculated to be $\Delta H^{\ddagger}$ = +37 kcal/mol and $\Delta S^{\ddagger}$ = +73 cal mol^{-1} K^{-1}. The similarity of the equilibrium and activation parameters for the $T_0 \rightarrow R_0$ transition indicates that the transition state is much more R-like than T-like. This result suggests that in the path from T_0 to R_0 the subunits have already almost completely rearranged into the R configuration when the transition state is reached, while in the path from R_0 to T_0 the subunits remain in a configuration close to R in the transition state. The finding of an R-like transition state explains why the binding of ligands causes much smaller changes in the R → T rates than in the T → R rates.

Upon deoxygenation tetrameric hemoglobins undergo a structural change consisting of a global rearrangement of the four subunits—the quaternary change—and widespread conformational changes within the individual subunits (Perutz, 1970; Baldwin & Chothia, 1979; Perutz et al., 1987). In the quaternary change the symmetrically related $\alpha\beta$ dimers rotate by about 15° relative to each other, resulting in atomic displacements at the intersubunit contacts of up to 6 Å (Baldwin & Chothia, 1979) (Figure 1). Recent X-ray studies also show that a change in ligation state in the absence of a quaternary conformational change results in tertiary conformational changes that are similar to, but smaller than, those associated with the quaternary transition (Makinen & Eaton, 1974;

* Author to whom correspondence should be addressed.
‡ Present address: Miles, Inc., Elkhart, IN 46515.
§ Permanent address: Department of Biochemical Sciences, University of Rome "La Sapienza", Piazzale A. Moro, 5, 00185 Rome, Italy.
∥ Fogarty Scholar-in-Residence, National Institutes of Health.